Effect of Substitution on the Optical Properties and HOMO−LUMO Gap of Oligomeric Paraphenylenes

Brian D. Koepnick,[‡,§] Jeremy S. Lipscomb,[†] and Darlene K. Taylor*[,†]

Department of Chemistry, North Carolina Central University, 3105 M. Townes Science Building, 1801 Concord Street, Durham, North Carolina 27707, United States, North Carolina School of Science and Math, 1219 Broad Street, Durham, North Carolina 27705, United States

Received: September 9, 2010; Revised Manuscript Received: October 16, 2010

A series of dialkyl amino benzophenone dimers with various alkyl chain lengths is presented. Gaussian B3LYP/6-31G(d) calculations show that the band gap decreases within the dimer series as a function of the donor group efficiency. Theoretical calculations show that the interaction between phenyl−phenyl rings is more important than simple donor−acceptor effects. We report the experimental and electro-optical properties of one of these dimers, *N*,*N*-(dibutyl)-4-amino-benzophenone. The experimental and theoretical results enabled us to design a new dimer. Altogether, side chain substituents reported herein tune the theoretical band gap of paraphenylene based dimers by over 8.86 eV.

Introduction

The potential for semiconducting polymers to outperform their silicon-based counterparts has inspired the development of organic-based solar cells,[1,2] light-emitting diodes (LEDs),[3−5] and photodetectors.[6] Modest progress in organic versions of these technologies has occurred through several strategies[7] that primarily utilize three small band gap materials platforms: aniline,[8] phenylene vinylene,[9−11] and thiophene.[12−16] Fundamental studies are needed to design better organic electronic materials. One approach widely overlooked in the literature is fundamental studies of high band gap polymers. Invaluable lessons can be learned about designing better semiconducting organic polymers by tuning high band gap polymers to push the boundaries of their wavelength absorption.

To this end, we have approached the field of organic electronic materials by focusing on paraphenylene oligomers and polymers. Oligomeric *para*phenylenes (OPP) are a class of organic semiconductors known for their excellent thermal and mechanical stability. Biphenyl is the simplest version of these molecules, but it is the para hexaphenyl version that has been widely reported for its optical properties and tested as an emitting layer in LEDs.[17−19] Fundamental studies on the electronic properties of hexa paraphenyls have emerged;[20] however, there are still unresolved structural questions pertaining to these highly luminescent materials and the class of paraphenylenes in general. Specific questions remain regarding the contributions of substitution on the phenyl ring and planarity between phenyl rings.

It is well established that side-chain substituent groups readily alter the conductivity of organic semiconductors;[21] however, little effort has been devoted to systematic structure−property relationships uniquely characterized by side chain substituted paraphenylenes. The positions of substituent groups along a polymer backbone as well as the number of substituent groups can affect conductivity. Studies have shown that adding two acceptor or donor groups to each fluorene−phenylene monomer unit has a greater effect on charge transfer in the resulting material.[22] Other studies on thiophenes have shown that large substituent groups tend to increase steric hindrance between monomer units. This potentially distorts the planarity of the dihedral angle and thus the π-orbital overlap between neighboring monomer units.[23]

On the basis of these facts and our ongoing interest in diethyl amino substituted poly(*p*-benzophenone),[24] we have chosen to alter systematically the side-chain substituent group of a series of paraphenlyene dimers as shown in Figure 1 to tune the resulting electrooptical properties. In all but one case, the substitution pattern involves either variations or replacement of the alkyl chains of the (dialkylamino) side-chain substituent. Theoretical studies show that the length of the alkyl chain group on the side-chain substituent group has very little effect on the electro-optical properties of the dimer series. However, a critical alkyl chain length of four carbons was apparent as dimer **A4** showed deviations in trends observed for the other dimers in series A. We prepared and characterized **A4** to confirm our theoretical observations. Experimental measurements of absorption, fluorescence emission, and redox potentials for dimer **A4** are reported. The results provide guidance for improving the design of paraphenylenes to produce more conductive materials. The possibilities are demonstrated in the case of **B2**, in which, in addition to dialkylamino substituents, the ketone functional group in the benzophenone unit has been replaced by a divinyl cyano substituent. Dimers **A0**, **A4**, **B0**, **B1**, and **B2** show theoretical optical absorption maxima that span over a modest 140.3 nm.

Experimental Methods

Theoretical Calculations. The geometrical and electronic properties of the substituted oligoparaphenylenes were performed with the Gaussian 03 program package.[25] The calculations were optimized by means of the Becke three-parameter hybrid functional with Lee−Young−Parr[26] correlation functional (B3LYP) using the 6-31G(d) basis set unless otherwise indicated. Molecular orbitals were visualized using WebMO. The theoretical absorption spectra of the dimers were calculated on

* To whom correspondence should be addressed. E-mail: dtaylor@nccu.edu.
‡ North Carolina School of Science and Math.
† North Carolina Central University.
§ Current address: Wake Forest University, Winston-Salem, NC 27106.

10.1021/jp108619n
Published on Web 11/19/2010

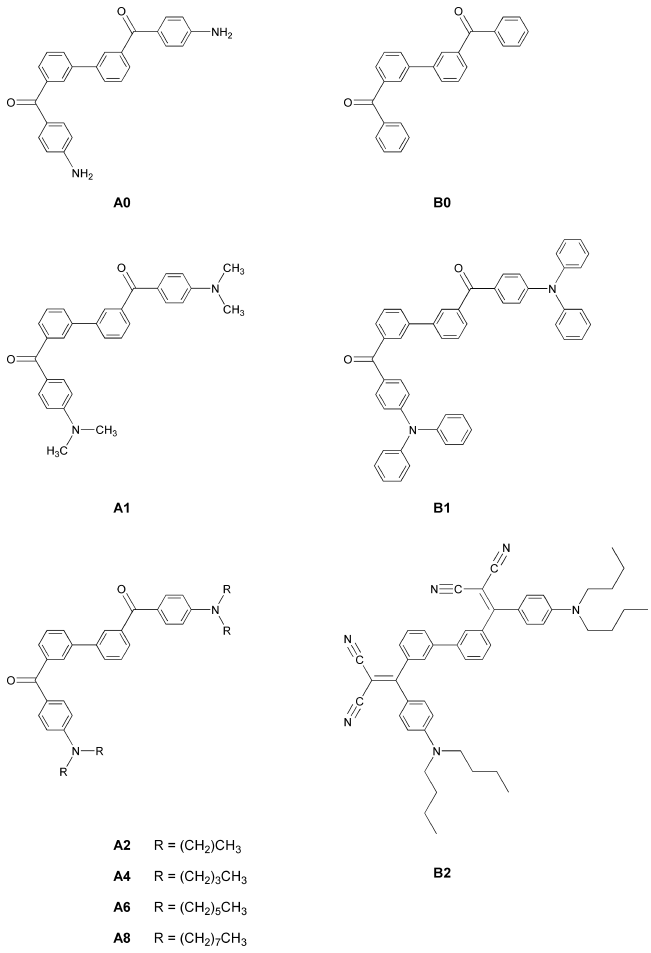

Figure 1. Structures of paraphenylene side-chain substituted dimers.

the B3LYP 6-31G optimized structures using the semiempirical method of Zerner's intermediate neglect of differential overlap (ZINDO).[27]

Instruments and Measurements. ^{1}H and ^{13}C NMR (300 MHz) spectra were measured on a Varian Inova spectrometer in deuterated chloroform. Chemical shifts (δ) for proton are reported in parts per million downfield from tetramethylsilane and are referenced to it (TMS 0.0 ppm). Coupling constants (J) are reported in Hertz. Chemical shifts for carbon are reported in parts per million downfield from TMS and are referenced to residual solvent peaks: carbon ($CDCl_3$, 77.0 ppm). Mass spectra were recorded on an Agilent Technologies 1200 series equipped with a XTerra MS (C-18, 5.0 μm) 3.0 × 100 mm column. Retention times (t_R) were obtained on the same instrument using HPLC/LC. Analytical thin-layer chromatography was performed on precoated 250 μm layer thickness silica gel 60 F 254 plates (EMD Chemicals Inc.). Visualization was performed with ultraviolet light. Elemental analysis was performed on Perkin-Elmer 2400 series II CHN analyzer.

Materials and Reagents. All materials were purchased from either Aldrich or Fisher and used without further purification unless otherwise noted. Tetrahydrofuran (THF) was freshly distilled prior to use. Bipyridine (Bipy) was purified by recrystallization from ethanol. Triphenylphosphine (TPP) was recrystallized from cyclohexane. Both reagents were dried under vacuum for 24 h at room temperature and stored in the glovebox under nitrogen. The catalyst, $(Ph_3P)_2NiCl_2$, and zinc (100 mesh, 99.999%) were also stored under nitrogen. Dimer **A4** was synthesized in a three-step process as shown in Scheme 1.

SCHEME 1: Synthesis of Dimer A4[a]

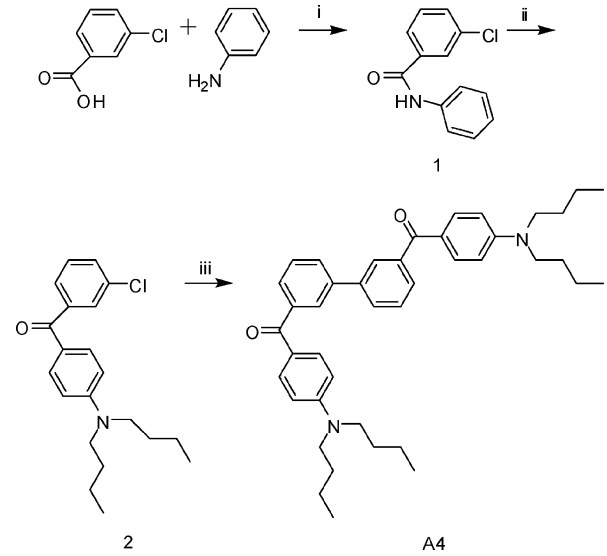

[a] Reagents and conditions: (i) 180 °C (neat); (ii) $POCl_3$, N, N-dibutylaniline, 100 °C; (iii) $(Ph_3P)_2$-$NiCl_2$, Zn, PPh_3, Bipy, THF, 60 °C.

3-Chloro-*N*-phenylbenzamide (1). The condensation of 3-chlorobenzoic acid (20 g, 130 mmol) with excess aniline (14.37 g, 154.3 mmol) yields the crude product. The excess aniline is removed by atmospheric distillation at 182 °C. The resulting solid is washed in acidic and basic aqueous solutions, and dried in vacuum after TLC showed complete absence of aniline. This reaction has shown product yields of up to 98%. The material is utilized without further purification.

(3-Chlorophenyl)(4-(dibutylamino)phenyl)methanone (2). The chlorinated monomer was prepared by a condensation reaction between **1** (16 mmol, 3.7 g) and *N*,*N*-dibutylaniline (53.5 mmol, 12.1 mL) in the presence of phosphorus oxychloride (22 mmol, 2.0 mL). An exothermic reaction was noted at around 80 °C before the reaction was cooled in an ice bath. The reaction was allowed to continue at 100 °C for 3 h. The crude resulting oil was stirred in 5% hydrochloric acid before it was washed with water. The organic product was taken up in ethyl acetate, dried over magnesium sulfate, and concentrated by rotovap to yield ~4 g of crude, brown, oily product. A crude product/silica mixture was prepared by dissolving the oil in ethyl acetate, mixing with silica (~100 mL), and evaporating the solvent. Meanwhile, a large column of silica (~180 g) slurried in cyclohexane was made up. The crude product/silica mixture was placed on top and eluted with ethyl acetate/cyclohexane (1:4), collecting 50 mL fractions. The first five fractions, identified by TLC to be purified product, were combined, and the solvent was removed in a vacuum to give a yellow oil. Yield: 2.47 g, 45%. ^{1}H NMR ($CDCl_3$, TMS, 300 MHz): δ 0.98 (t, 6H, $J = 6$ Hz), 1.36 (sextuplet, 4H, $J = 6$ Hz), 1.6 (quintuplet, 4H, $J = 6$ Hz), 3.55 (t, 4H, $J = 6$ Hz), 6.62 (d, 2H, $J = 9$ Hz), 7.36 (t, 2H, $J = 6$ Hz), 7.47 (dd, 1H, $J_1 = 2$ Hz, $J_2 = 7$ Hz), 7.58 (dd, 1H, $J_1 = 2$ Hz, $J_2 = 7$ Hz), 6.68 (d,1H, $J = 2$ Hz), 7.94 (d, 2H, $J = 9$ Hz). APCI/ESI-MS: m/z 344.2 $[M - H]^-$, $t_R = 9.36$ min.

Biphenyl-2,3′-diylbis((4-(dibutylamino)phenyl)methanone) (A4). A previously flame-dried, three-neck, 100 mL, round-bottom flask equipped with a magnetic stir bar was charged with 0.589 g (9.01 mmol, 3.1 equiv) of zinc, 0.380 g (0.581 mmol, 0.2 equiv) of $(Ph_3P)_2-NiCl_2$ catalyst, 0.152 g (0.581 mmol, 0.2 equiv) of triphenylphosphine (TPP), and

0.0454 g (0.291 mmol, 0.1 equiv) of bipyridine (Bipy). The reagents were combined in the glovebox under a nitrogen atmosphere. The flask was sealed with rubber septa, purged with nitrogen, and charged with 6 mL of THF via syringe. The catalyst mixture was stirred and heated in an oil bath at 50 °C under the nitrogen purge. Once the color of the catalyst mixture changed from deep green to dark red, 1.0 g (9.0 mmol) of monomer dissolved in 3 mL of THF was added via syringe. The reaction continued at 50 °C overnight. The reaction mixture was then washed with 5% HCl solution to remove excess zinc and stirred overnight. The product was taken up in ethyl acetate, dried over magnesium sulfate, and concentrated by rotovap. The crude product was separated from TPP by flash column using cyclohexane as an elutant. Once TLC confirmed the absence of TPP from the elutant, a brown band containing dimer and unreacted monomer was flash-eluted using ethyl acetate. Silica was added, and a crude product/silica mixture was obtained by rotovaporation to remove the solvent. Meanwhile, a column of silica (~90 g) slurried in cyclohexane was made up. The crude product/silica mixture was placed on top and eluted with ethyl acetate/cyclohexane (1:4), collecting 50 mL fractions. The column was followed by TLC, the first several fractions were combined, and the solvent was removed in vacuo to give yellow crystals. Yield: 45%. Anal. Calcd for ($C_{42}H_{52}N_2O_2$): C, 81.78; H, 8.50; N, 4.54; O, 5.19. Found: C, 81.68; H, 8.47; N, 4.61. ^{1}H NMR ($CDCl_3$, TMS, 300 MHz): $\delta = 0.962$ (t, 12H, $J = 7$ Hz), 1.36 (sextet, 8H, $J = 7$ Hz), 1.605 (quintet, 8H, $J = 8$ Hz), 3.34 (t, 8H, $J = 7$ Hz), 6.64 (d, 4H, $J = 8$ Hz), 7.528 (t, 2H, $J = 8$ Hz), 7.841 (m, 8H), 7.9 (s, 2H). ^{13}C NMR ($CDCl_3$, 300 MHz): $\delta = 14.2$, 20.5, 29.5, 51.1, 110.5, 123.9, 128.2, 128.8 (d, $J = 17.4$ Hz, C_{aryl}), 129.97, 133.3, 140.5 (d, $J = 51.9$ Hz, C−C), 151.8, 194.8 (CO). UV−vis [methanol, λ_{max} (ε)]: 245 (1.83), 369 (2.26). APCI/ESI-MS: m/z 617.4 $[M - H]^-$, $t_R = 8.53$ min.

Optical Spectroscopy. Absorption spectra of dimer **A4** in solution were measured with a Hewlett-Packard model 8453 UV−vis spectrophotometer with HP Vectra Workstation. The fluorescence spectra of dimer **A4** were observed on a Perkin-Elmer LS 55 fluorescence spectrometer at ambient temperature. In both absorbance and emission spectra, the samples were contained in 1-cm path-length quartz cells.

Electrochemistry. Cyclic voltammograms were recorded using a BAS potentiostat (CV-50W with C3 cell stand) interfaced to a personal computer and software supplied by the manufacturer. Acetonitrile (anhydrous, 99.8%, ≤0.001% water content) was obtained from Aldrich and used as received. Tetrabutylammonium hexafluorophosphate (Bu_4NPF_6) and ferrocene were recrystallized several times from freshly distilled THF using Schlenck line techniques. All experiments were conducted in 0.1 M Bu_4NPF_6 in CH_3CN under ambient laboratory conditions. A working volume of 5 mL was transferred to the cell by syringe immediately prior to the start of the experiment.

A normal one-compartment cell was utilized with a Pt disk working electrode (MF-2013, BAS), a Pt wire auxiliary electrode (MW-1032), and a Ag/AgCl reference electrode (MF-2052, BAS). The silver reference electrode was calibrated against the redox potential of ferrocene/ferrocenium ion (evaluated as the average of $E_{pa} = 0.609$ V and $E_{pc} = 0.514$ V) as the internal standard in an identical cell without sample. No electroactive species were observed in the potential range of interest (0.0−1.5 V vs Ag/AgCl) in the absence of ferrocene. All potentials are reported vs Ag/AgCl. Electrochemical potentials were converted to vacuum assuming the normal hydrogen electrode (NHE) to be at 4.7 eV vs vacuum with an additional +0.2 V potential difference between Ag/AgCl and NHE. Before each experiment, the cell was purged with N_2 for 5−10 min, and a blanket of N_2 was maintained during the experiment.

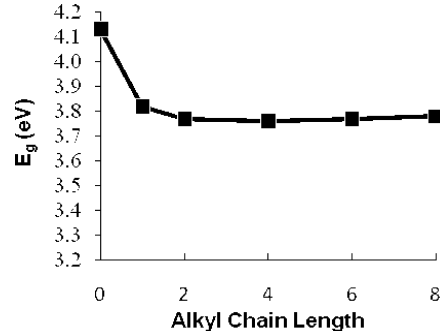

Figure 2. Influence of alkyl chain length (n) on band gap of the six dimers in series **A*n*** (where $n = 0$, 1, 2, 4, 6, or 8).

TABLE 1: The Band Gaps (E_g) by B3LYP/6-31G of Various Substituted Paraphenylene Dimers

dimer	coupling[a]	E_g (eV)
A0	TT	4.13
	HT	3.92
A1	TT	3.82
A2	TT	3.77
	HT	3.74
A4	TT	3.76
	HT	3.82
A6	TT	3.77
	HT	3.86
A8	TT	3.78
	HT	3.79
B0	TT	4.52
	HT	4.59
B1	TT	3.54
B2	TT	1.17

[a] TT = tail-to-tail; HT = head-to-tail.

Results and Discussion

Band Gap Calculations of Series A Dimers. The theoretical band gap (E_g) is the transition energy required to excite electrons from the ground state to the first dipole-allowed excited state. A crude and widely accepted[28−30] estimate of this quantity is the energy difference between the highest occupied molecular orbital (HOMO) and the lowest unoccupied molecular orbital (LUMO). The energy of the HOMO or LUMO level can be altered by substituents. Figure 2 shows that in going from an amino side group (**A0**) to a (diethylamino) side group (**A2**), the band gap is lowered by 0.36 eV. This behavior is a result of the electron-releasing effect created by the introduction of the alkyl side chains. Further increase in the number of carbon atoms (n) has no effect on the resulting E_g.

It should be noted that this study has focused on the tail-to-tail (TT) coupling of dimers shown in Figure 1. However, geometry optimization calculations were also performed for select head-to-tail (HT) dimer molecules (structures not shown), and the computed band gaps were very similar to those reported for the TT verison (see Table 1). This suggests that HT and TT coupling have very little effect on the resulting bandgap, and others have reported similar findings for poly(benzo-2,1,3-thiadiazol-4,7-diyl)-(dihexyl[2,2′]dithiophene-5,5′-diyl).[31] Apparently, the critical number of carbon atoms in the **A*n*** dimer series is $n = 4$. Butyl and higher alkyl chain side groups induce

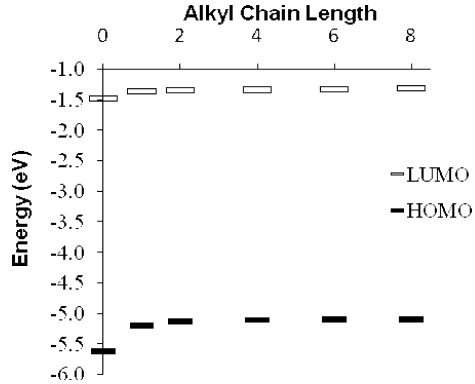

Figure 3. Influence of alkyl chain length (n) on HOMO and LUMO in series **A*n*** (where $n = 0$, 1, 2, 4, 6, or 8).

SCHEME 2: Dihedral Angle, φ, between Monomer Units

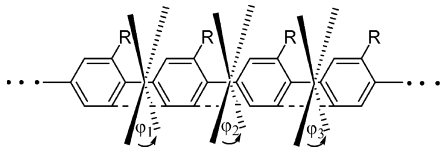

a competing steric hindrance effect that negates any further increase in the energy of the HOMO (see Figure 3).[32] The side chain dialkylamino substituents have no effect on the energetic position of the LUMO. The combined effect is an unaltered E_g for **A4**, **A6**, and **A8**.

The band gap is also expected to be affected by the torsion between adjacent monomer units. This is denoted as φ_n in Scheme 2. An ideal spatial alignment is obtained when $\varphi_n = 0$, but this is rarely observed, since the side chain groups introduce repulsive or attractive forces that twist the phenyl−phenyl ring alignment away from planarity. For the **A*n*** dimers under investigation, the average dihederal angle is 38°. It is surprising that the addition of carbon atoms in the side chain dialkyl amino group (i.e., the bulking up of the side chain appendage with $n = 0-8$) has very little effect on the respective φ_n. There is, however, a small but noticeable peak in the dihedral angle when going from dimer **A2** to **A4** (see Figure 4). To evaluate the significance of this increase in φ, select versions of the dimers in the **A*n*** series were extended to longer oligomer lengths; energy minimization calculations were performed on $\mathbf{A0_x}$, $\mathbf{A2_x}$, and $\mathbf{A4_x}$ at the B3LYP/3-21G level of theory where $x = 2$ and 4 (i.e., tetramer and ocatomer oligomer analogues). The calculations showed that the range of dihedral angles within a given tetramer increased as the alkyl chain length increased in going from $\mathbf{A0_2}$ (52−55°) to $\mathbf{A2_2}$ (54−58°) to $\mathbf{A4_2}$ (37−56°). This

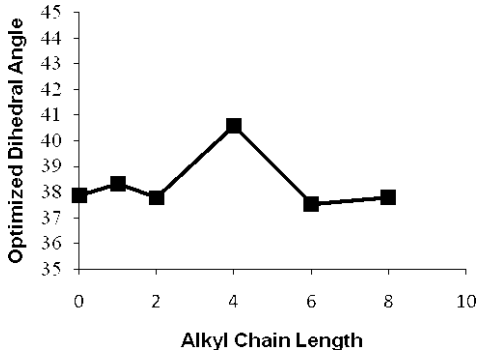

Figure 4. Torsional angle between monomer units of dimers in series **A** as a function of alkyl side chain group.

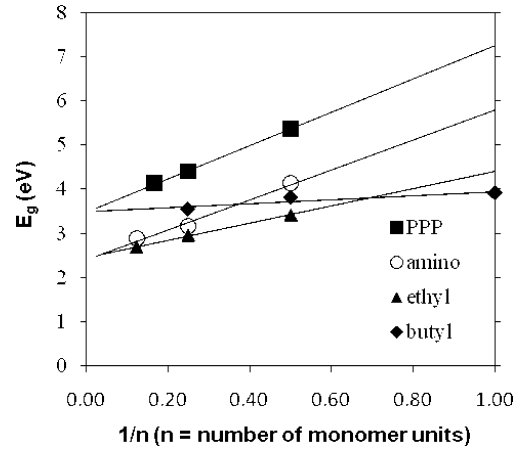

Figure 5. Band gaps for infinite chain unsubstituted paraphenylene (PPP) and amino, diethylamino, and dibutyl amino substituted versions of parabenzophenone were determined by plotting band gaps in respective oligomers against the inverse of the number (n) of monomer units and extrapolating the number of units to infinity.

trend was also observed in the octamer analogs, where the six dihedral angles of $\mathbf{A0_4}$ spanned fewer degrees than the six dihedral angles of $\mathbf{A2_4}$ (i.e., $\Delta\varphi_{A0} < \Delta\varphi_{A2}$). We conclude that the more dihedral angles present in the chain, the more likely the range of dihedral angles will increase. It would be beneficial to understand how φ_n is effected by interchain packing in $\mathbf{A4_4}$. Others have observed that increasing the oligomer length in unsubstitued paraphenylenes (PPP) resulted in an increased interchain packing and thus a decreased torsion angle as one progressed from diphenyl and terphenyl (45−50°)[17]to hexaphenyl (30−40°).[33]

The band gap of monomer, dimer (**A4**), and tetramer oligomers of dibutyl amino benzophenone were extrapolated to determine theoretical estimates for the band gap of the corresponding polymer. Figure 5 shows that the electrical properties of poly(dibutyl amino benzophonone) ($E_g = 3.4$ eV) are similar to that of unsubstituted poly(paraphenylene) ($E_g = 3.5$ taken from the literature)[34] and higher than poly(diethyl amino benzophenone) ($E_g = 2.5$ eV) or poly(aminobenzophenone) ($E_g = 2.4$ eV). These values have been calculated by plotting band gaps of energy-minimized oligomers against the inverse of the number (n) of monomer units and extrapolating the number of units to infinity. For the oligomers reported here, we conclude that the steric interaction of the side groups on the phenyl rings dominate the distorted backbone geometry more than the stabilizing effects gained by the electrons being delocalized over a planar backbone. The net effect is that the π-overlap between monomer units decreases, leading to a decreased bandwidth and thus an increased band gap.

Although not a large difference, the 3° increase in optimal dihedral angle configuration for the **A4** dimer over all other dimers in the **A** series led to a closer examination of this molecule. The dihedral angle of **A4** was fixed at various values; the optimized geometry was calculated, followed by a calculation of the MO energies to calculate the band gap as a function of torsional angle. Figure 6 shows that the minimal band gap for the essentially planar **A4** molecule is 3.74 eV and increases to a maximum value of 3.92 eV as the dihedral angles increase to 180°. The optimal dihedral angle for **A4** is 40°, resulting in a band gap of 3.76 eV. This is very similar to the band gap reported by Zade et al. for the unsubstituted poly(paraphenylene) (3.78 eV).[35] This again leads to the conclusion that **A4** exhibits little improvement over PPP. It can be concluded that the

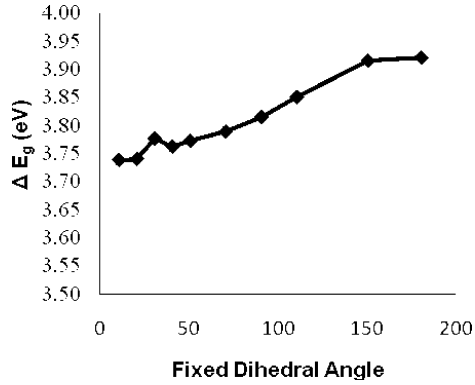

Figure 6. Band gap energy calculated for **A4** as a function of fixed dihedral angle.

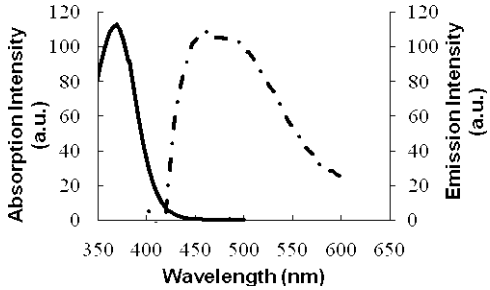

Figure 7. Optical absorption spectrum (—) and fluorescence emission spectrum (— •) of oligomer **A4** dissolved in methanol.

electron-releasing effect on the energy of the HOMO of **A4** has a smaller influence on band gap than steric hindrance of the side chain group.

Experimental Calculations of Band Gap for A4. We report the first experimental determination of the optical bandgap in semiconducting **A4** dimers. The target dimer was synthesized as presented in Scheme 1. The absorption and emission spectra are overlaid in Figure 7. The UV−vis absorption spectrum of **A4** has no structural features and shows a maximum absorption at 369 nm. This value was used to determine the optical HOMO−LUMO gap (E_g^{opt} = 3.37 eV).

Unlike the absorption spectrum, the fluorescence emission spectrum is structured. A broad peak centered at 460 nm is observed to have a weak shoulder at long wavelength. The single site substitution on the phenyl backbone is the most likely reason for the assymmetric emission peak structure. Beljonne et al.[36] have observed similar effects in their substituted oligothiophenes and concluded that the structured emission spectra were due to a more planar conformation in the excited state dimer.

The energy level of the electronic states of the HOMO and LUMO can be studied using electrochemistry. The electrochemical properties of dimer **A4** were investigated by cyclic voltammetry, and the results are shown in Figure 8. More than one peak is observed in the voltammogram. This is quite common, and others have attributed this to the formation of polarons followed by bipolarons.[37] The potential for the oxidation peak was extracted from the first sweep and found to be 0.48 V versus Ag/AgCl. Electrochemical potentials were converted to vacuum assuming the normal hydrogen electrode (NHE) to be at 4.7 eV vs vacuum with an additional +0.2 V potential difference between Ag/AgCl and NHE. Thus, the energetic position of the HOMO level is 5.2 V. We were unable to obtain any reduction processes for dimer **A4** and, therefore, cannot report on the electrochemically determined LUMO level.

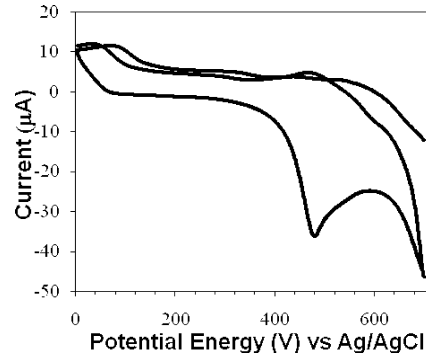

Figure 8. Cyclic voltammogram of 0.8 mM A4 in 0.1 M Bu_4NPF_6/CH_3CN.

TABLE 2: Summary of Absorption and Emission Data for Dimer A4

λmax abs (nm)	λmax emis (nm)	E_g^{opt} (eV)[a]	E_{HOMO}^{El} (eV)[b]	E_g^{th} (eV)[c]
368	460	3.37	5.20	3.74

[a] Optical band gap derived from the absorption (λ_{max} = 368 nm) of the solution spectrum. [b] Electrochemically derived energy position of the HOMO band. [c] Theoretical calculation of band gap.

The data compare very well with the values of optical and theoretical band gap discussed previously. A summary of the electrooptical properties for dimer **A4** is presented in Table 2.

Enhancing the Paraphenylene Platform. From the combined theoretical and experimental studies, we set out to explore substituent groups that more effectively lowered the band gap of oligoparaphenylenes. Table 1 shows that 2,2′-(biphenyl-3,3′-diylbis((4-(dibutylamino)phenyl)methan-1-yl-1-ylidene))dimalononitrile (**B2**) has the lowest calculated band gap of the dimers under investigation. Although the electron-donating substituent group is unchanged between **A4** and **B2**, the calculated HOMO level is raised by 0.62 eV in the latter. The calculated LUMO level is lowered by 1.97 eV by changing the ketone in **A4** to a divinyl cyano group. The combined effect is a significantly lower calculated band gap for **B2** that deviates from expectations based on a simple donor−acceptor effect. With no change in the donor part of the dimer, altering the acceptor group in **B2** should mainly affect the LUMO. The reduction of the band gap in dimer **B2** consisting of divinyl cyano groups must be attributed to the combined effect of a better electron acceptor [CO versus C═C−(C′N)$_2$] as well as a further extension of the π-conjugation. Furthermore, calculated optical absorption of **B2** provides a significant red shift from **A4**. The dimers **A0**, **A4**, **B0**, **B1**, and **B2** together span a modest 140.3 nm window, from 238.9 to 379.2 nm. The successful tuning of the theoretical absorption maxima (see Figure 9) is promising and suggests that substituents can be designed to enhance the electrooptical properties of paraphenylenes.

Conclusions. We have prepared a substituted polyparaphenylene dimer that looked promising from initial design and theoretical calculations. On closer investigation, this dimer and the others within this series that we chose to investigate showed only modest improvements over the unsubstituted poly(paraphenylenes). The alkyl chain length on the side chain substituent group was found to have very little effect on the calculated HOMO−LUMO band gaps or torsional angles between monomer units of the dimers. We were, however, successful at showing theoretically that a divinyl cyano version of our dimers has a lower band gap and a red shift in the optical absorption. This is a successful outcome for this class of materials that will be explored experimentally in future studies.

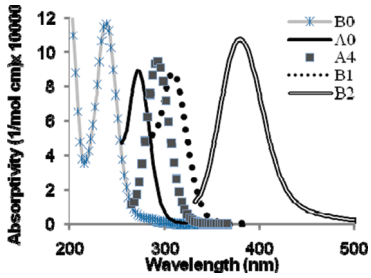

Figure 9. Calculated absorption spectra of dimers **A0**, **A4**, **B0**, **B1**, and **B2**. The geometry optimizations were carried out with DFT (B3LYP 6-31G) methods, and the theoretical spectra of the dimers under study were obtained with ZINDO methods.

Acknowledgment. This work was supported by the Petroleum Research Fund of the American Chemical Society (No. 45702-GB10). The authors thank the Cluster Computing Group at Earlham College and the Shodor Education Foundation for computational server time.

References and Notes

(1) Brabec, C. J.; Sariciftci, N. S.; Hummelen, J. C. *Adv. Funct. Mater.* **2001**, *11*, 15–26.
(2) Hoppe, H.; Sariciftci, N. S. *J. Mater. Res.* **2004**, *19*, 1924–1945.
(3) Barbarella, G.; Melucci, M.; Sotgiu, G. *Adv. Mater.* **2005**, *17*, 1581–1593.
(4) Ho, P. K. H.; Kim, J.-S.; Burroughes, J. H.; Becker, H.; Li, S. F. Y.; Brown, T. M.; Cacialli, F.; Friend, R. H. *Nature* **2000**, *404*, 481–484.
(5) Perepichka, I. F.; Perepichka, D. F.; Meng, H.; Wudl, F. *Adv. Mater.* **2005**, *17*, 2281–2305.
(6) Heeger, A. J.; Diaz-Garcia, M. A. *Curr. Opin. Solid State Mater. Sci.* **1998**, *3*, 16–22.
(7) Forrest, S. R. *MRS Bull.* **2005**, *30*, 28–32.
(8) Wallace, G. G.; Dastoor, P. C.; Officer, D. L.; Too, C. O. *Chem. Innovation* **2000**, *30*, 14–22.
(9) Braun, D.; Heeger, A. J. *Appl. Phys. Lett.* **1991**, *58*, 1982–1984.
(10) Friend, R. H.; Gymer, R. W.; Holmes, A. B.; Burroughes, J. H.; Marks, R. N.; Taliani, C.; Bradley, D. D. C.; Dos Santos, D. A.; Brédas, J. L.; Logdlung, M.; Salaneck, W. R. *Nature* **1999**, *397*, 121–128.
(11) Remmers, M.; Neher, D.; Gruner, J.; Friend, R. H.; Gelinck, G. H.; Warman, J. M.; Quattrocchi, C.; dos Santos, D. A.; Bredas, J. L. *Macromolecules* **1996**, *29*, 7432–7445.
(12) Hou, J.; Tan, Z.; Yan, Y.; He, Y.; Yang, C.; Li, Y. J. *J. Am. Chem. Soc.* **2006**, *128*, 4911–4916.
(13) Hou, J. H.; Huo, L. J.; He, C.; Yang, C. H.; Li, Y. F. *Macromolecules* **2006**, *39*, 594–603.
(14) Karsten, B. P.; Viani, L.; Gierschner, J.; Cornil, J.; Janssen, R. A. *J. Phys. Chem. A* **2009**, *113*, 10343–10350.
(15) Karsten, B. P.; Viani, L.; Gierschner, J.; Cornil, J. R. M.; Janssen, R. A. J. *J. Phys. Chem. A* **2008**, *112*, 10764–10773.
(16) Leclerc, M. *Adv. Mater.* **1999**, *11*, 1491–1498.
(17) Baker, K. N.; Fratini, A. V.; Resch, T.; Knachel, H. C.; Adams, W. W.; Socci, E. P.; Farmer, B. L. *Polymer* **1993**, *34*, 1571–1587.
(18) Greta, G.; Leditzky, G.; Ullrich, B.; Leising, G. *Syn. Metals* **1992**, *51*, 383–389.
(19) Hosokawa, C.; Higashi, H.; Kusumoto, T. *Appl. Phys. Lett.* **1993**, *62*, 3238–3241.
(20) Graupner, W.; Meghdadi, F.; Leising, G.; Lanzani, G.; Nisoli, M.; De Silvestri, S.; Fischer, W.; Stelzer, F. *Phys. Rev. B* **1997**, *56*, 10128.
(21) Mammo, W.; Admassie, S.; Gadisa, A.; Zhang, F.; Inganaes, O.; Andersson, M. R. *Sol. Energy Mater. Sol. Cells* , *91*, 1010–1018.
(22) Zeng, G.; Chua, S.-J.; Huang, W. *Thin Solid Films* **2002**, *417*, 194–197.
(23) Iraqi, A.; Barker, G. W.; Pickup, D. F. *React. Funct. Polym.* **2006**, *66*, 195–200.
(24) Taylor, D. K.; Samulski, E. T. *Macromolecules* **2000**, *33*, 2355–2358.
(25) Frisch, M. J.; Trucks, G. W.; Schlegel, H. B.; Scuseria, G. E.; Robb, M. A.; Cheeseman, J. R.; Montgomery, J. A.; Vreven, T.; Kudin, K. N.; Burant, J. C.; Milam, J. M.; Iyengar, S. S.; Tomasi, J.; Barone, V.; Mennucci, B.; Cossi, M.; Scalmani, G.; Rega, N.; Petersson, G. A.; Nakatsuji, H.; Hada, M.; Ehara, M.; Toyota, K.; Fukuda, R.; Hasegawa, J.; Ishida, M.; Nakajima, T.; Honda, Y.; Kitao, O.; Nakai, H.; Klene, M.; Li, X.; Knox, J. E.; Hratchian, H. P.; Cross, J. B.; Adamo, C.; Jaramillo, J.; Gomperts, R.; Stratmann, R. E.; Yazyev, O.; Austin, A. J.; Cammi, R.; Pomelli, C.; Ochterski, J. W.; Ayala, P. Y.;; Morokuma, K.; Voth, G. A.; Salvador, P.; Dannenberg, J. J.; Zakrzewski, V. G.; Dapprich, S.; Daniels, A. D.; Strain, M. C.; Farkas, O.; Malick, D. K.; Rabuck, A. D.; Raghavachari, K.; Foresman, J. B.; Ortiz, J. V.; Cui, Q.; Baboul, A. G.; Clifford, S.; Cioslowski, J.; Stefanov, B. B.; Liu, G.; Liashenko, A.; Piskorz, P.; Komaromi, I.; Martin, R. L.; Fox, D. J.; Keith, T.; Al-Laham, M. A.; Peng, C. Y.; Nanayakkara, A.; Challacombe, M.; Gill, P. M. W.; Johnson, B.; Chen, W.; Wong, M. W.; Gonzalez, C.; Pople, J. A.; Gaussian, Inc.: Pittsburgh, PA, 2003.
(26) Lee, C.; Yang, W.; Parr, R. G. *Phys. Rev. B* **1988**, *37*, 785–789.
(27) Ridley, J.; Zerner, M. C. *Theor. Chim. Acta (Berlin)* **1973**, *32*, 111–134.
(28) Kertesz, M.; Choi, C. H.; Yang, S. *Chem. Rev.* **2005**, *105*, 3448–3481.
(29) Salzner, U.; Pickup, P. G.; Poirier, R. A.; Lagowski, J. B. *J. Phys. Chem. A* **1998**, *102*, 2572–2578.
(30) Yang, S.; Olishevski, P.; Kertesz, M. *Synth. Met.* **2004**, *141*, 171–177.
(31) Bundgaard, E.; Krebs, F. C. *Polym. Bull.* **2005**, *55*, 157–164.
(32) Winder, C.; Sariciftci, N. S. *J. Mater. Chem.* **2004**, *14*, 1077–1086.
(33) Tsuzuki, S.; Tanabe, K. *J. Phys. Chem.* **1991**, *95*, 139–144.
(34) Bredas, J. L.; Chance, R. R.; Silbey, R.; Nicolas, G.; Durand, P. *J. Chem. Phys.* **1982**, *77*, 371–378.
(35) Zade, S. S.; Bendikov, M. *Org. Lett.* **2006**, *8*, 5243–5246.
(36) Beljonne, D.; Meyers, F.; Brédas, J. L. *Synth. Met.* **1996**, *80*, 211–222.
(37) Guay, J.; Diaz, A. F.; Bergeron, J.-Y.; Leclerc, M. *J. Electroanal. Chem.* **1993**, *361*, 85–91.

JP108619N